

Intracellular Fluid Mechanics: Coupling Cytoplasmic Flow with Active Cytoskeletal Gel

Alex Mogilner^{1,2} and Angelika Manhart¹

¹Courant Institute of Mathematical Sciences, New York University, New York, NY 10012;
email: mogilner@cims.nyu.edu, angelika.manhart@cims.nyu.edu

²Department of Biology, New York University, New York, NY 10012



ANNUAL REVIEWS **Further**

Click here to view this article's online features:

- Download figures as PPT slides
- Navigate linked references
- Download citations
- Explore related articles
- Search keywords

Annu. Rev. Fluid Mech. 2018. 50:347–70

First published as a Review in Advance on October 13, 2017

The *Annual Review of Fluid Mechanics* is online at fluid.annualreviews.org

<https://doi.org/10.1146/annurev-fluid-010816-060238>

Copyright © 2018 by Annual Reviews.
All rights reserved

Keywords

actin, active polar gel, blebs, cytoplasmic fluid flow, free moving boundary, myosin

Abstract

The cell is a mechanical machine, and continuum mechanics of the fluid cytoplasm and the viscoelastic deforming cytoskeleton play key roles in cell physiology. We review mathematical models of intracellular fluid mechanics, from cytoplasmic fluid flows, to the flow of a viscous active cytoskeletal gel, to models of two-phase poroviscous flows, to poroelastic models. We discuss application of these models to cell biological phenomena, such as organelle positioning, blebbing, and cell motility. We also discuss challenges of understanding fluid mechanics on the cellular scale.

CELL MECHANICS

The cell, the fundamental unit of life, is first and foremost a biochemical reactor and a self-replicating carrier of hereditary information (Alberts et al. 2014). The idea that the cell is also a mechanical machine changing shape and generating movements and forces is also well accepted and growing in recognition of its importance (Iskratsch et al. 2014). The mechanical aspects of cell life are central for cell motility, cell division, intracellular transport, and positioning of organelles, to name but a few relevant phenomena.

The cytoskeleton, a dynamic network of polymers cross-linking proteins and molecular motors, is the main part of the cellular mechanical machine (Alberts et al. 2014). The discrete nature of the molecular elements of the cytoskeleton has drawn much attention to the view of the cell as a dynamic machine built from interconnected, solid, deformable and force-generating molecular units. However, on the scale of the whole cell, much insight comes from treating the cytoskeleton as a continuous gel (Pollack 2001). The cytoskeletal gel is highly nontrivial for two reasons: First, because it is active in the sense discussed below, and second, because its mechanical properties are very complex.

Another important aspect of the cell is that it is filled with cytoplasm, a fluid that permeates the cytoskeletal scaffold. Organelles and large protein complexes either float in the cytoplasm or are embedded in the cytoskeletal mesh. There is a certain confusion related to the notion of the cytoplasm: The term is used both for the fluid fraction of the cell interior and the whole mixture of the fluid and cytoskeletal mesh in the cell. Also, there exists a mild controversy about the fluid versus gel-sol or colloidal nature of the cytoplasm (reviewed in Luby-Phelps 2013). To avoid confusion, in this review we try to avoid the term cytoplasm and use the term cytosol to describe the fluid fraction of the cytoplasm. The mechanical role of the cytosol is less well studied than that of the cytoskeleton. In recent years, though, it has become clear that the intimate connection between the interpenetrating cytoskeletal mesh and cytosol plays an important role in many cell mechanical phenomena.

Quantitative analysis of the cell mechanics created exciting new computational problems, and, in turn, mathematical models of the cell fluid dynamics made a significant impact on understanding of experimental data. Here, we review mathematical and computational models of cell mechanics, starting with hydrostatics and Stokes flows of the cytosol in a cell volume devoid of a cytoskeleton and, in contrast, moving to models of the cell cytoskeleton as an active gel, ignoring the cytosol. Then we proceed to the full complexity of the two-phase flow models that consider interdependent dynamics of the cytoplasm and of an either viscous or elastic cytoskeletal gel.

In this review, we discuss only the cell mechanics above the molecular scale. There is a great wealth of interesting fluid mechanics phenomena on the molecular scale (tens of nanometers), for example, growth of a single actin filament in fast fluid flow (Carlier et al. 2014), as well as relevant computational modeling (Goldstein 2016); here, we consider mechanics only on the scale of the whole cell (tens of microns). Similarly, we do not consider the fluid dynamics of multicellular groups on the tissue scale (Lee & Wolgemuth 2011, Peskin & McQueen 1995) or the fluid mechanics of blood flow (Kamm 2002). Many aspects of fluid mechanics on the cellular scale have been reviewed earlier, including multiphase flow theories and biofilms (Cogan & Guy 2010), mechanics of red blood cells and platelets, the response of endothelial cells to blood flow (Kamm 2002), cilia- or flagella-related fluid dynamics (Eloy & Lauga 2012, Goldstein 2016), leukocyte rolling under the action of flow and dynamic adhesions (Khismatullin & Truskey 2012), and cell swimming (Schwarz 2015). We touch only lightly on the electrolyte aspects of cell mechanics; readers can find deeper coverage of this topic by Tao et al. (2017). We discuss a few recent studies of cytoplasmic streaming; further and more extensive discussion can be gleaned from Goldstein &

van de Meent (2015). Goldstein (2016) provided an elegant and exciting review of the history of fluid dynamics in biology. Even with all these restrictions, it is impossible to cite all computational studies of cell-related fluid dynamics, and for that, we apologize in advance.

CHARACTERISTIC MECHANICAL SCALES IN THE CELL

A majority of animal cells, which are the focus of our discussion, have a characteristic linear size in the range of tens of microns (Alberts et al. 2014). Characteristic rapid cell movement rates are on the order of $\sim 0.1\text{--}1 \mu\text{m/s}$ (Keren et al. 2009); hence, the characteristic relevant time is minutes. Fluid cytosolic flow rates, in the few cases when they were directly or indirectly measured, are $\sim 0.1\text{--}1 \mu\text{m/s}$ (Keren et al. 2009), and sometimes are greater in larger cells at $\sim 1\text{--}10 \mu\text{m/s}$ (Lewis et al. 2015). Slower flows on the order of $\sim 0.01 \mu\text{m/s}$ were also detected (Yi et al. 2011). Rates of molecular motors' movement and of cytoskeletal fibers' growth, which in most cases ultimately generate the flows, are also in the $\sim 0.1\text{--}1 \mu\text{m/s}$ range (Gross et al. 2000). Motor-generated rates of deformation and displacement of the cytoskeleton mesh are, again, on the same order or slower (Keren et al. 2009). Organelle movement in the cell is normally slow at $\sim 1 \mu\text{m/min}$ (Yi et al. 2011).

On the microscopic (nanometer) scale, the viscosity of the cytosol is similar to that of water, $\sim 10^{-3} \text{ Pa}\cdot\text{s}$. However, at greater scales, due to crowding of the cytoplasm and many complex physico-chemical factors, the effective viscosity of the cytoplasm is likely an order (or even two orders) of magnitude higher, $\sim 10^{-2}\text{--}10^{-1} \text{ Pa}\cdot\text{s}$ (Luby-Phelps 1999). The mesh size of the actin network is in the range of tens of nanometers (Charras et al. 2005, Keren et al. 2009), and therefore the diffusion of a majority of globular proteins, $\sim 10 \text{ nm}$ in size, is sensitive to the local conditions in the cell. For example, the effective diffusion coefficient of actin monomers could be as low as $\sim 1 \mu\text{m}^2/\text{s}$ (Keren et al. 2009), more than an order of magnitude less than the diffusion coefficient of this protein in water.

These characteristic scales lead to the extremely low Reynolds numbers, $\sim 10^{-5}$. Even in giant cells with faster flows, the Reynolds numbers are still much smaller than 1 (Goldstein 2016). Therefore, inertial terms can safely be neglected in all cell biology-relevant problems, and Stokes flow is an accurate approximation for the cytosol. In contrast, Péclet numbers characterizing the effectiveness of the convective mode of transport, as compared to diffusion, could be on the order of 1 (or greater, or smaller). Thus, effectiveness of the cytosolic flow for intracellular transport has to be investigated on a case-by-case basis.

Fluid pressure inside the cell is normally $\sim 100 \text{ Pa}$ higher with respect to that of the external fluid (Charras et al. 2008). This pressure is the result both of myosin-generated squeezing of the cytosol by the contracting actomyosin mesh (Keren et al. 2009) and of the osmotic pressure generated by much higher ion concentration in the cell compared to the outside aqueous medium (Tao et al. 2017); both factors could be on the same order of magnitude. Hydraulic permeability of the cytoskeletal mesh can be estimated by the mesh size, viscosity of the cytosol, and volume fraction of the cytosol. In cells, the latter varies significantly but is generally on the order of tens of percentage points (Luby-Phelps 1999), and hence, the hydraulic permeability of the cytoskeleton is on the order of $0.1 \mu\text{m}^4/(\text{pN}\cdot\text{s})$ (Charras et al. 2005, Keren et al. 2009). Thus, a characteristic pressure gradient of $\sim 10^2 \text{ Pa}$ over $10 \mu\text{m}$ can generate $\sim 1 \mu\text{m/s}$ flow, as observed. Similarly, viscous friction between the cytoskeletal mesh and the cytosol squeezing through it is comparable to the magnitude of the motor- or polymer-generated stresses. The membrane lipid bilayer is largely impermeable to water; however, the plasma membrane contains aquaporins that increase the permeability dramatically. One estimate of the permeability of a cell membrane with aquaporins is $\sim 10^{-5} \mu\text{m}^3/(\text{pN}\cdot\text{s})$ (Keren et al. 2009); hence, the characteristic pressure drop across the

cell boundary can generate fluid flow on the order of 10^{-3} – 10^{-2} $\mu\text{m}/\text{s}$. However, concentrating aquaporins in specific locations can increase the membrane permeability, and thus the flow from and into the cell by another order of magnitude (Keren et al. 2009).

Characteristic active stress inside the cytoskeletal mesh can be estimated by measuring traction forces that the cell applies to the substrates. Many measurements consistently give estimates of hundreds of pascals (Lewis et al. 2015, Oakes et al. 2014), consistent with estimates of hundreds of molecular motors, each producing a piconewton range force, per square micron of the cytoskeletal network (Robinson & Spudich 2004, Wollman et al. 2008). Pressure of the same order of magnitude can be generated at the cell surface by actin polymerization (Prass et al. 2006).

A great deal of experimental and theoretical research has been devoted to the material properties of the cytoskeleton. The widely accepted view is that the cytoskeleton is viscoelastic (Bausch & Kroy 2006); specifically, it is elastic on short timescales, when elastic actin and microtubule polymers are firmly and densely cross-linked into the coherent mesh by a vast host of cross-linking proteins, and viscous on long timescales, when the cross-linking proteins dissociate, allowing the mesh to remodel and cross-link again. The characteristic turnover time of individual cross-linkers is on the order of seconds (Alberts et al. 2014); interestingly, a few experimental studies estimated the relaxation time, at which elastic behavior turns into a viscous one, to be in the range of seconds (Kole et al. 2005). The relaxation time can likely vary from tenths to tens of seconds from cell to cell. Existential measurements of the elastic Young modulus of the cytoskeleton provide estimates in the range of 10^3 – 10^4 Pa (Charras et al. 2005, Rotsch et al. 1999). Viscosity of the actin network was estimated to be on the order of 10^3 Pa·s (Bausch et al. 1998), orders of magnitude higher than that of the cytosol.

The estimates above allow us to answer the following basic question: Are intracellular fluid mechanics an important part of cell mechanics? The general answer is yes, because (*a*) the characteristic osmotic/hydrostatic pressure of cytosol is of the same order of magnitude as the cytoskeleton-generated stresses; (*b*) rates of fluid flow are often as fast as rates of cell movements; (*c*) convection is often as effective as diffusion in intracellular transport; and (*d*) viscous friction between the solid and fluid fractions of the cytoplasm is comparable to the cytoskeletal stresses. Often, a specific cell geometry allows either a focus on the cytoskeletal mechanics, neglecting the effects from the cytosol (Rubinstein et al. 2009), or concentration on the cytosolic forces, omitting the cytoskeletal mechanics (Dai & Sheetz 1999). However, it is becoming increasingly clear that in many cell biological phenomena, the mechanics of the cytoskeleton and cytosol are intimately intertwined. Below, we review recent studies on which this view is based.

HYDROSTATICS OF BLEBS AND THE OSMOTIC ENGINE MODEL

We start with mathematically straightforward examples that are very important for cell biological applications, where hydrostatics or extremely simple cytoplasmic flows underlie important cell mechanical phenomena. One of these examples is the early model of blebs (Sheetz et al. 2006) that emerged from pioneering experiments measuring membrane tension by the laser tweezer-powered pulling of membrane tethers from the blebs (Dai & Sheetz 1999). Blebs (**Figure 1a**) are small, dynamic, hemispherical blisters of the membrane (Charras et al. 2005, Tinevez et al. 2009). Originally, blebbing was thought to be a functionless process accompanying cell apoptosis, but a growing number of recent studies have suggested that it plays an important role in cell locomotion (Bergert et al. 2012, Diz-Muñoz et al. 2016, Paluch & Raz 2013).

Initially, the membrane is attached to the underlying actin cortex through adhesion proteins. Myosin contracts the actin cortical mesh, leading to tension in the cortex and effectively pressurizing the cytoplasm. The resulting hydrostatic pressure generated by the actomyosin cortex

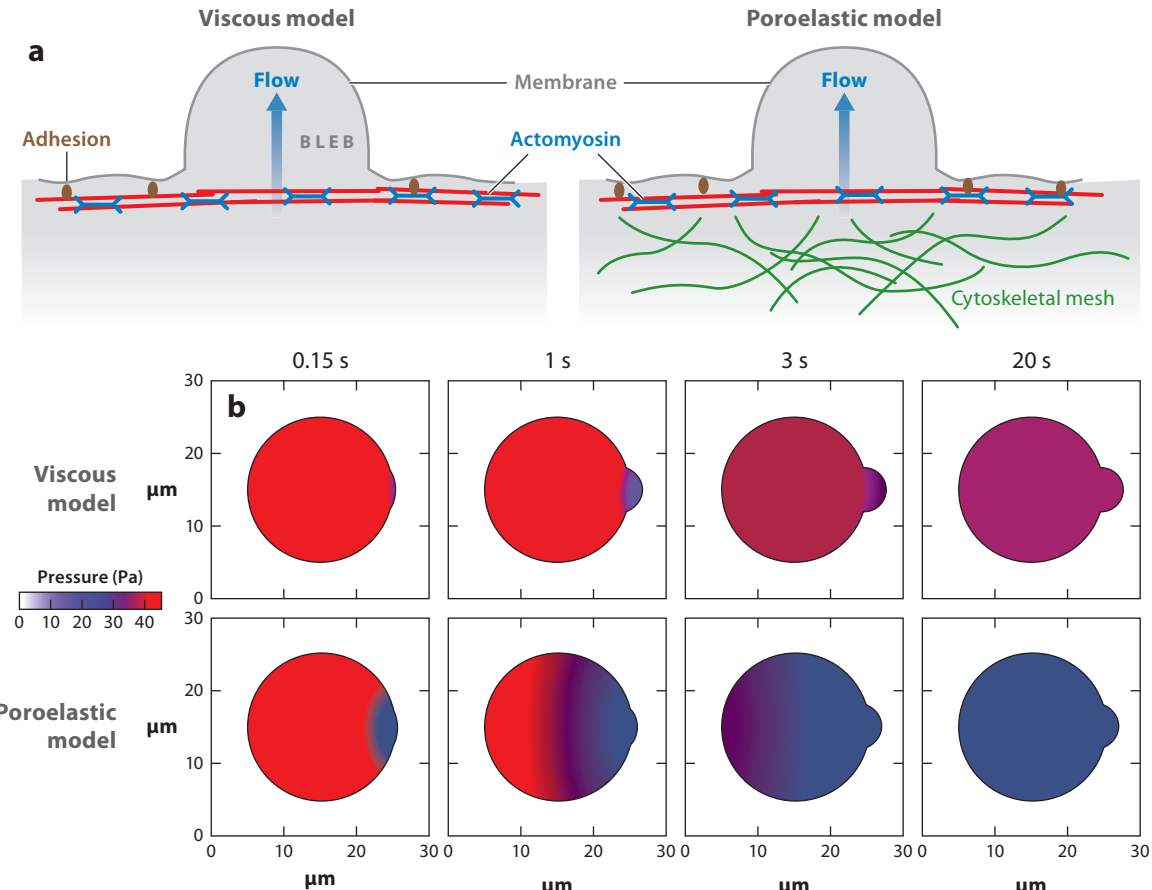


Figure 1

Blebbing. (a) Bleb formation is initiated by a disruption of the adhesions (brown) between the actomyosin cortex, with actin in red and myosin in dark blue, and the membrane (gray). In the viscous model (left), the cytoplasm is treated as a simple viscous fluid, whereas, in the poroelastic model (right), the cytoskeletal mesh is treated as a separate (elastic) phase. (b) Comparison of the viscous and poroelastic models. The colors represent hydrostatic pressure. In the poroelastic model (bottom row), the pressure gradient extends across the entire cell and changes with time, whereas, in the viscous scenario (top row), it remains more localized near the bleb. Also, in the viscous model, the final pressure relief by bleb expansion is much lower than in the poroelastic model. Adapted with permission from Strychalski & Guy (2016).

tension, likely assisted by the osmotic pressure inside the cell, stretches the plasma membrane and generates the in-plane membrane tension, not to be confused with the cortical tension. The bleb's life cycle is thought to start from a local decoupling of the cortex from the membrane (Figure 1a). The hydrostatic/osmotic pressure then delaminates the membrane from the cortex and drives the cytosol into the growing bleb, a hemispherically shaped extension (Figure 1a). The bleb growth is resisted and eventually stopped by the plasma membrane tension and curvature. After a brief mechanical equilibrium, the actomyosin cortex reassembles in the bleb and adheres to the membrane, and eventually the cortical contraction retracts the bleb. Alternatively, the nascent cortex in the bleb is not contractile, and the bleb becomes a stable protrusion from the cell surface.

The simplest way to understand the bleb expansion is to assume that both the hydrostatic/osmotic pressure and the membrane tension are constant in time and space. Laplace's law,

$P = 2T/R$, where $P \sim 100 \text{ pN}/\mu\text{m}^2$ is the pressure, $T \sim 100 \text{ pN}/\mu\text{m}$ is the tension, and $R \sim 1 \mu\text{m}$ is the bleb's radius, says that for the bleb of the characteristic radius to appear, the threshold hydrostatic/osmotic pressure of the cytoplasm has to be exceeded, and removal of adhesions from a membrane patch of a critical radius has to occur for the bleb to grow (Sheetz et al. 2006).

Even earlier than the surge of attention to the blebbing phenomenon, there were proposals that the osmotic pressure can drive the protrusion at the leading edge of the motile cell (Oster & Perelson 1987). It was proposed that the elastic cross-linked gel of electrically charged cytoskeletal fibers effectively immobilizes otherwise mobile counter ions in the cytosol and keeps the osmotic pressure at the cell leading edge low. Partial de-cross-linking and disassembly of the gel frees a fraction of the small ions, leading to an increase in the osmotic pressure, influx of water through the semipermeable membrane, and swelling of the cell leading edge.

The Oster–Perelson model requires a relatively complex cytoskeletal behavior. Recently, it was shown both experimentally and theoretically, following earlier ideas about osmotic-based protrusion (Jaeger et al. 1999), that a cell can crawl through a narrow channel in the absence of the cytoskeleton (Stroka et al. 2014). The respective model is that of the osmotic engine (**Figure 2b**): Cells can maintain a polarized distribution of ion exchangers and aquaporin channels. Such a polarized distribution leads to different ion fluxes at the cell front and rear, creating a gradient of the osmotic pressure from front to rear. By solving simple equations for the diffusion of ions and for the Stokes flow of the cytosol in the cell, Stroka et al. (2014) showed that this gradient causes water to be sucked into one end of the cell and expelled from the other, generating the cell movement. The osmotic engine model also predicted that a nonzero cell velocity can be achieved in confined spaces as a result of different extracellular osmolarities at the cell's leading and trailing edges, and thus a hypotonic shock at the leading edge or a hypertonic shock at the trailing edge of the cell may reverse the direction of cell migration. This prediction was confirmed experimentally (Stroka et al. 2014). It is also interesting to note that a relevant qualitative nuclear piston model was recently proposed by Petrie et al. (2014): Actomyosin contraction pulls the nucleus—squeezed between the cell sides in the dense extracellular matrix—forward, which pressurizes the cytosol at the cell front, and the resulting pressure generates the protrusion.

An interesting twist on the osmotic engine model is provided by analysis of a situation in which the membrane is permeable to positive but not to negative ions (Li et al. 2015). Simple analysis shows that if an electric field is imposed on a cell so that the voltage is higher at the back, a current carried by positive ions will flow through the cell from back to front. This current together with the electroneutrality condition produces a gradient of the intracellular solute concentration, resulting in a global osmotic water flow that propels the cell (Li et al. 2015). Cells migrate directionally in electric fields, and although the engine of this migration is usually the actomyosin gel, and the electric field is but the directional cue (Allen et al. 2013), it is feasible that the field-generated osmotic flows can drive the cell.

CYTOPLASMIC FLOW GENERATED BY ACTIVE CYTOSKELETAL ELEMENTS

The next level of computational complexity occurs when there is a nontrivial flow of the cytosol but no small-meshed cytoskeletal scaffold permeating the volume of the cell. Rather, the main bulk of the cytoskeleton is concentrated in the cortex—a relatively thin ($\sim 1 \mu\text{m}$) band at the cell boundary, underlying the plasma membrane. Movements of actin or microtubule fibers in the cortex and/or molecular motors on these fibers then create boundary conditions, generating a flow of the cytoplasm in the cell volume. One example of such models is the description of the cell plasma membrane as an elastic contour, underlined by another elastic contour that represents the

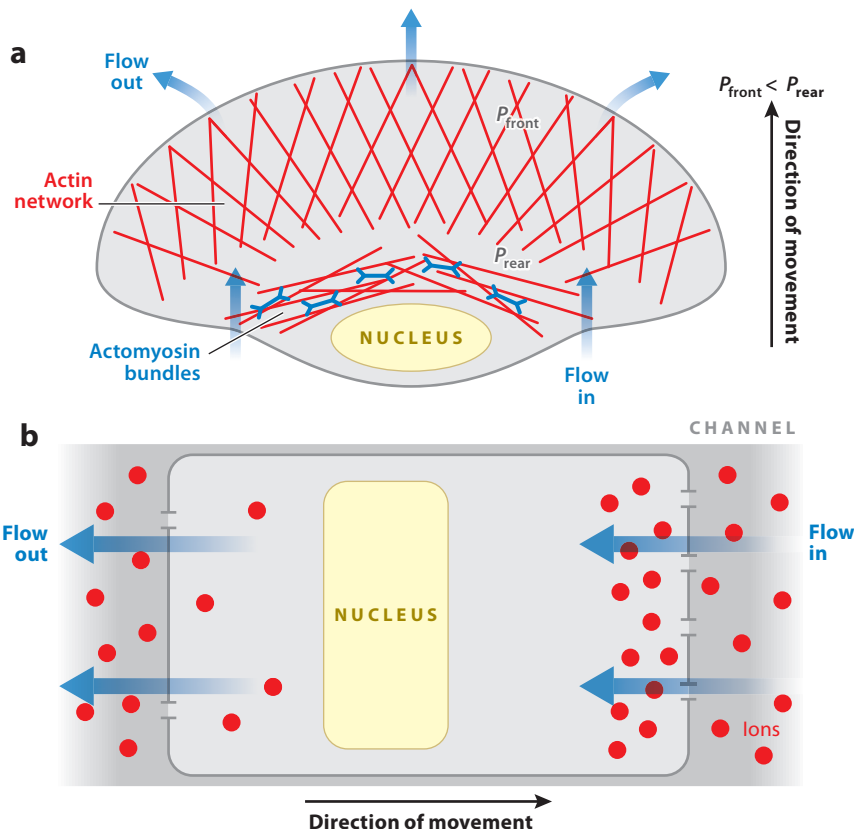


Figure 2

Fluid flow through moving cells. (a) Model for fluid flow in moving keratocyte (Keren et al. 2009). The front (top) of the moving keratocyte is dominated by an actin network (red), the main component of the lamellipodium. At the rear, contractile bundles are formed by actin (red) and myosin (blue). The contraction at the rear of the keratocyte creates a hydrostatic pressure gradient between the rear and the front. Consequently, fluid flows from the outside of the cell through the rear, toward the leading edge and out of the cell (blue arrows). (b) Osmotic engine model (Stroka et al. 2014). A cell confined to a thin channel has an asymmetric distribution of ion channels and aquaporins. A polarized distribution of ions (red) within the cell is thereby established. The resulting osmotic pressure gradient causes water (blue arrows) to enter at the leading end (right) and leave at the trailing edge (left), resulting in the cell moving in the opposing direction, to the right.

actin cortex, which is contractile due to myosin action. Another important component is adhesive elastic links between the cortex and membrane contours. Models of this kind were recently used to investigate the role of the cytosol, modeled as a Newtonian fluid, in bleb formation (Lim et al. 2012, Strychalski & Guy 2012, Young & Mitran 2010).

Strychalski & Guy (2012), for example, treated the cortex as a permeable membrane that experiences a drag as it moves through the cytoplasm and used the framework of the immersed boundary method (Peskin & McQueen 1995) to simulate the model of the coupled cytosol and cortex mechanics. In this model, the only sources of intracellular drag are shear in the cytosol and friction between the cortex and the cytosol flowing through it. A bleb was initiated by removing the membrane-cortex adhesions in a small region. This causes a local transient drop of the hydrostatic

pressure, generating a local cytosolic flux that inflates the bleb. In this model, the timescale of bleb inflation is dominated by the drag between the cytosol and cortex and not fluid viscosity. Simulations showed that in order for the bleb to form on the observed timescale, the value of the drag coefficient between the cytosol and cortex has to be very high, which is achievable only with a cortical mesh size that is an order of magnitude smaller than has been observed experimentally. This result indicates that a viscous fluid model of the cytoplasm is not fully adequate to describe the blebbing cells.

Following the experimental finding that blebbing can play a role in cell migration (Bergert et al. 2012), Lim et al. (2013) used a model similar to that of Strychalski & Guy (2012) to demonstrate that a blebbing cell confined in a channel can move. In this model, the cell squeezed between the channel walls becomes cylindrical, with hemispherical front and rear. When adhesions between the cortex and membrane elastic contours break at the front, the membrane locally deforms outward and the cytosol rushes into the protruding bleb. As a result, the cortex tension increases a little, which effectively contracts the cell rear pulling it forward. Even though there is also a slight retraction at the leading edge, the overall effect is a small forward translocation of the cell. To end the cell motility cycle, the membrane–cortex adhesions at the leading edge reform, and the cell is ready for a new blebbing–protrusion–retraction event.

In much larger cells, such as oocytes of *Drosophila* and *C. elegans*, viscous flow of the cytosol is similarly believed to be powered by an actomyosin cortex or movements of motors on microtubules. This flow is responsible for transporting mitochondria, RNA, and other organelles and molecules (Quinlan 2016, Wolke et al. 2007). Cytoplasmic streaming in giant cells has been reviewed extensively (Goldstein 2016, Goldstein & van de Meent 2015); here, we highlight but a few recent studies.

The origin of the cytoplasmic streaming in *Drosophila* oocytes was recently clarified computationally by Monteith et al. (2016) (**Figure 3c**). Following multiple observations, the authors posited that most microtubules are anchored with their minus ends at the oocyte cortex and extend their plus ends inward, forming a dynamic three-dimensional (3D) meshwork. Kinesin motors walk toward the microtubule plus ends dragging the cytosol with them, effectively pushing microtubules toward their minus ends, resulting in buckling. Initially, the meshwork of microtubules stays disordered, generating minor, slow cytoplasmic flows. Subsequently, the cytosol and the microtubule layer self-organize so that the microtubules form parallel bending arrays that support long-range, fast flows that facilitate mixing in a low-Reynolds-number regime (**Figure 3c**). Similar mathematics and computations were applied to show the effect of cytoplasmic flows and diffusion on the formation of a Bicoid morphogen gradient in the early *Drosophila* embryo (Hecht et al. 2009, Trong et al. 2015, Xie & Hu 2016).

Different kinds of motors on a different microtubule array were recently proposed to position an important organelle in the *C. elegans* embryo (Shinar et al. 2011) (**Figure 3a**). The male pronucleus in this cell is a spherical body bound to two microtubule-organizing centers; minus ends are anchored at the pronucleus, whereas dynamic, growing, and shortening plus ends emanate outward. Shinar and coworkers tested the idea that dynein motors walking and carrying cargo toward the minus ends drag the incompressible Newtonian fluid, namely, cytosol, constrained within an ellipsoidal eggshell. Simulations using the immersed boundary formulation demonstrated that the balance of Stokes flows, generated by the motors along the microtubules to the pronucleus, and of viscous drag is sufficient to move the pronucleus to the cell center. Effectively, the motor-generated flow along each microtubule is proportional to the length of the fiber. Consequently, if the pronucleus is near one side of the cell, then microtubules extending to the opposite side are long, and the forces they generate are large and direct the pronucleus away from the proximal side (**Figure 3a**).

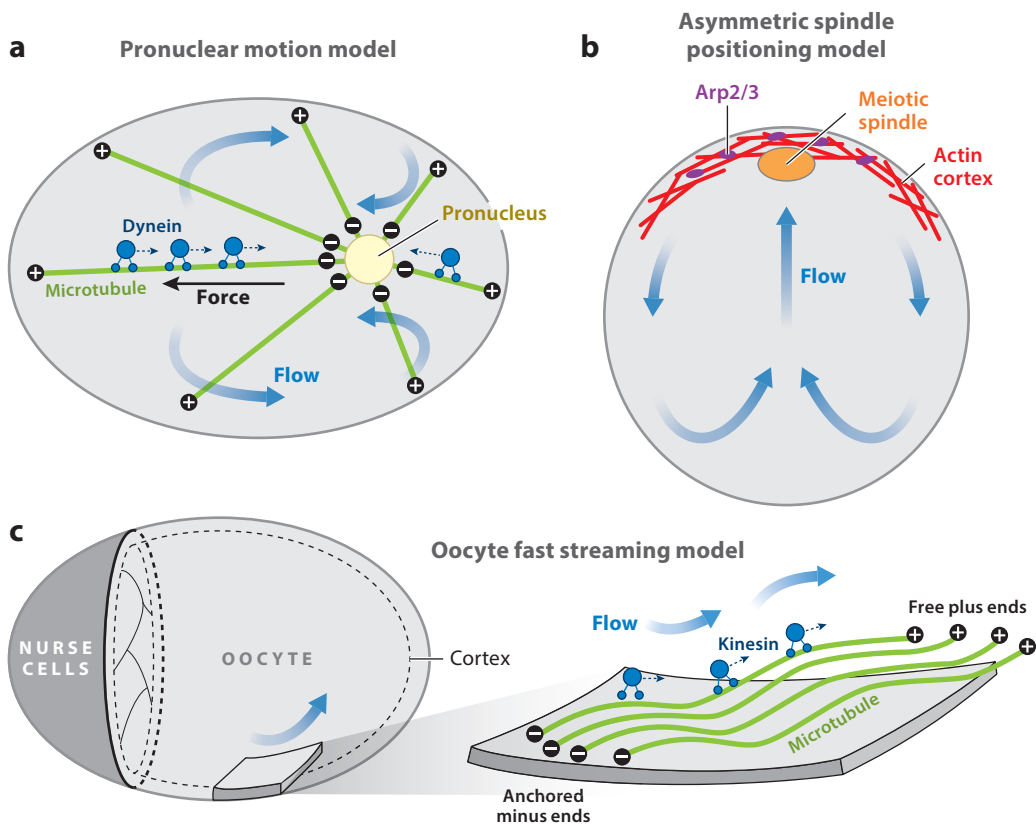


Figure 3

Cytoplasmic flow caused by cytoskeletal components. (a) Model for pronuclear motion (Shinar et al. 2011). Microtubules (green), with their plus ends facing toward the cell membrane, are anchored with their minus ends to the male pronucleus (yellow) in the *Caenorhabditis elegans* embryo. Dynein motors (dark blue) attach to the microtubules and move toward the minus ends. Due to the viscosity of the cytosol, this exerts a length-dependent pulling force on the pronucleus, which leads movement to the left and hence to centering. The resulting flow in the early stages of this movement is depicted in blue. For simplicity, we show only one microtubule aster. (b) Model for asymmetric spindle positioning (Yi et al. 2011). In the depicted mouse oocyte, Arp2/3 complexes (purple) are localized by the spindle to the cortical cap (top of cell) and nucleate an actin network (red). Actin filaments move along the sides of the cell, radially and downward, to the opposing pole. This causes cytoplasmic streaming (blue arrows) following the actin flow near the boundary. The flow returns upward along the cell axis and pushes the meiotic spindle (orange) to the cortical cap. (c) Model for fast streaming in oocytes (Monteith et al. 2016). During late *Drosophila* oogenesis, nurse cells (left side of ellipsoid) squeeze their cytoplasm into the oocyte (right side of ellipsoid). Subcortical microtubules (green) have their minus ends tethered to the oocyte's cortex. Kinesin motors (dark blue) move toward the free plus ends, thereby causing a cytoplasmic flow (blue arrows), which synchronizes the microtubule movement to form sinusoidal, parallel waves. The resulting long-ranging, fast cytoplasmic streaming helps to mix the cytosolic components of the oocyte.

Another elegant example of the organelle positioning, shown in **Figure 3b**, that uses a physically similar yet molecularly very different mechanism was unraveled in a combined experimental/theoretical study by Yi et al. (2011). In mouse oocytes, asymmetric divisions require the meiotic spindle to be positioned close to the cortical region, near the “North Pole” of the big, fluid cytoplasm-filled cell. Yi and coworkers discovered that it is not microtubules but the actin cortex, without assistance from myosin, that generates the cytoplasmic flows that keep the spindle near the cell pole. In this process chromosomes in the spindle activate the signaling protein Ran,

which indirectly localizes and activates the Arp2/3 complex that governs the growth of the actin network at the proximal cortex. As a result, the actin network starts to treadmill along the inner cell surface, from the North Pole radially outward and down toward the cell equator. This actin flow at the surface creates the boundary condition for the cytosol. Solution of the equation for the Stokes flow shows the ensuing fountain flow that moves from the North to the South Pole close to the surface and returns from the South to the North Pole at the cell center (**Figure 3b**). It is precisely this South-North flow at the center that keeps the spindle near the North Pole. Hence, in the same fashion as that of the microtubule-based model of Shinar et al. (2011), the self-organization of the flow and organelle-centered cytoskeletal activity leads to robust organelle positioning.

ACTIVE GEL THEORY AND ACTOMYOSIN FLOW

In many cases, the cytosol is neglected in cell mechanics models, and researchers focus on cytoskeletal mechanics. On the timescales relevant for cell migration, the actin network exhibits a slow, creeping flow, indicating that viscous effects are dominant. However, it is rarely clear whether elastic effects can be ignored. Therefore, a viscoelastic description of the actin network is often used. Broadly speaking, a general model of cell migration consists of force balance and mass conservation equations for key molecular concentrations. First, active and passive forces have to be balanced. In the context of cell migration, the two active forces consuming energy from ATP hydrolysis and/or protein binding are the pushing/swelling force generated by growing actin filaments and the contractile force generated by myosin motors. Mathematically, the respective stresses are similar to a pressure term in hydrodynamics equations, where polymerization forces would lead to an effectively positive and myosin forces to an effectively negative pressure. Three other forces are passive (i.e., they dissipate or conserve energy): the traction force from the drag between the cytoskeleton and adhesion complexes on the substrate, membrane tension resisting the polymerization force, and viscoelastic stresses from deformations in the actin network. The mass conservation equations on which constitutive relations of the cell mechanics depend are typically reaction-diffusion-drift equations for key molecular concentrations. The constitutive relations include, for example, dependencies of the contractile stress on the myosin density and of the actin network viscosity on the actin density.

A pioneering discrete 1D model of a migrating cell was a serial chain of Kelvin elements (elastic springs and viscous dashpots in parallel) together with contractile elements. Similar continuous models introduced later considered both elastoviscous (springs and dashpots in parallel, hence the actin network does not flow on long timescales) (Gracheva & Othmer 2004, Larripa & Mogilner 2006), viscoelastic (springs and dashpots in series, hence the actin network flows on long timescales) (Kruse et al. 2006, Rubinstein et al. 2009), purely elastic (Rubinstein et al. 2005), and purely viscous (Barnhart et al. 2015, Carlsson 2011, Recho et al. 2013) models of the crawling cells. An insightful illustration that viscoelastic effects can lead to nontrivial patterns in the actomyosin continuum was given by Lewis et al. (2014), who showed that in the emerging pattern in a contractile gel, one region can be dominated by viscous and another by elastic forces.

Some of these models imposed a polarization on the cell, for example, by polarized boundary conditions ensuring extension at the front and retraction at the rear. Others, interestingly, predicted a self-polarization of the initially symmetric cell. This was the case, for example, in the model of Barnhart et al. (2015), in which it was posited that the viscous, compressible actin gel is contracted by the myosin stress, which is proportional to the local myosin density, and the effective

viscous drag between the gel and the substrate limits the actin flow generated by the contraction. The governing equations take the form

$$\underbrace{[(\mu_b + \mu/3)\nabla\nabla \cdot \mathbf{U} + \mu\nabla^2\mathbf{U}]}_{\text{viscous stress in actin network}} + \underbrace{k\nabla M}_{\text{myosin contractile stress}} = \underbrace{\zeta\mathbf{U}}_{\substack{\text{adhesion} \\ \text{viscous drag}}} - \underbrace{\frac{\partial M}{\partial t}}_{\substack{\text{myosin diffusion}}} = \underbrace{D\nabla^2 M}_{\text{myosin diffusion}} - \underbrace{\nabla \cdot (\mathbf{U}M)}_{\text{myosin drift with actin flow}},$$

where \mathbf{U} is the actin flow velocity and M is the myosin density, and they were complemented by the zero stress and zero myosin flux conditions at the boundary. In the equations, μ and μ_b are actin viscosities, k is the myosin strength coefficient, ζ is the adhesion viscous drag coefficient, and D is the effective myosin diffusion coefficient.

The model showed that when myosin starts to aggregate to the center, the myosin density gradient generates centripetal actin flow, which transports more myosin to the center. This positive feedback leads to myosin accumulation at the center and radially symmetric actin centripetal flow, keeping the cell symmetric. Barnhart et al. (2015) discovered experimentally that the adhesions showed stick-slip behavior; that is, they are strong for slow and weak for fast actin flows: $\zeta = \zeta_1$ for $|\mathbf{U}| < U_0$, $\zeta = \zeta_2$ for $|\mathbf{U}| > U_0$, $\zeta_1 \gg \zeta_2$. This feature of the flow-dependent adhesion strength was added to the model of the initially symmetric cell with the free boundary. Numerical simulations showed that when the initial condition was asymmetric—adhesion strength decreased at a random side of the cell—the centripetal flow at that side accelerated, and the boundary at that side, the prospective rear, was retracted by the flow. The cell started to move in the direction opposite to that side. The movement led to myosin being swept to the rear, which stabilized the movement by keeping the flow fast at the rear and locking the adhesion there in the slipping state, whereas at the front adhesion remained sticking, allowing the protrusion at the leading edge to extend the boundary.

Most models built by adding active stresses to traditional viscoelastic theories are isotropic. This presents a problem because the cytoskeleton is markedly anisotropic due to the polarity of actin and microtubule filaments. A generic hydrodynamic theory describing active, polar gels that relies only on symmetry arguments was developed to address this difficulty (Joanny & Prost 2009; Kruse et al. 2004, 2005). According to this theory, active polar gels are viscoelastic materials formed by polar filaments and maintained in a nonequilibrium state by the actin treadmilling, microtubule dynamic instability, and myosin motor action. Mathematically, the key feature of the theory is the dynamic orientation field added to the hydrodynamics with active stresses. The essential property of active polar gels turned out to be the ability to flow spontaneously even in the absence of any external force. This property was used to model several cell motility-related phenomena, for example, chimneying, the self-propulsion of an active cytoskeletal gel strip in an undulating channel (Zumdieck et al. 2008). Chimneying may be relevant to 3D cell migration through the porous extracellular matrices. Another notable application of active gel theory was to explain the shape of the dorsoventral (vertical) cross section of the lamellipodium and the correct reproduction of the observed retrograde actin flow in this motile appendage (Kruse et al. 2006).

Recently, an exciting application of active gel theory to the self-organization of the mitotic spindle, the molecular machine that segregates chromosomes in dividing cells, demonstrated that the spindle that is normally thought of as an elastic cage made of long microtubules can be considered as a fluid if individual microtubules are much shorter than the whole spindle (Brugués et al. 2012). The model simulations reproduced the correct spindle shape, polarity, and flow distribution observed in experiments (Brugués et al. 2012). Very recently, it was observed experimentally that small blobs of cross-linked actin gel also behave as polar fluid droplets and form spindle-like particles (Weirich et al. 2017).

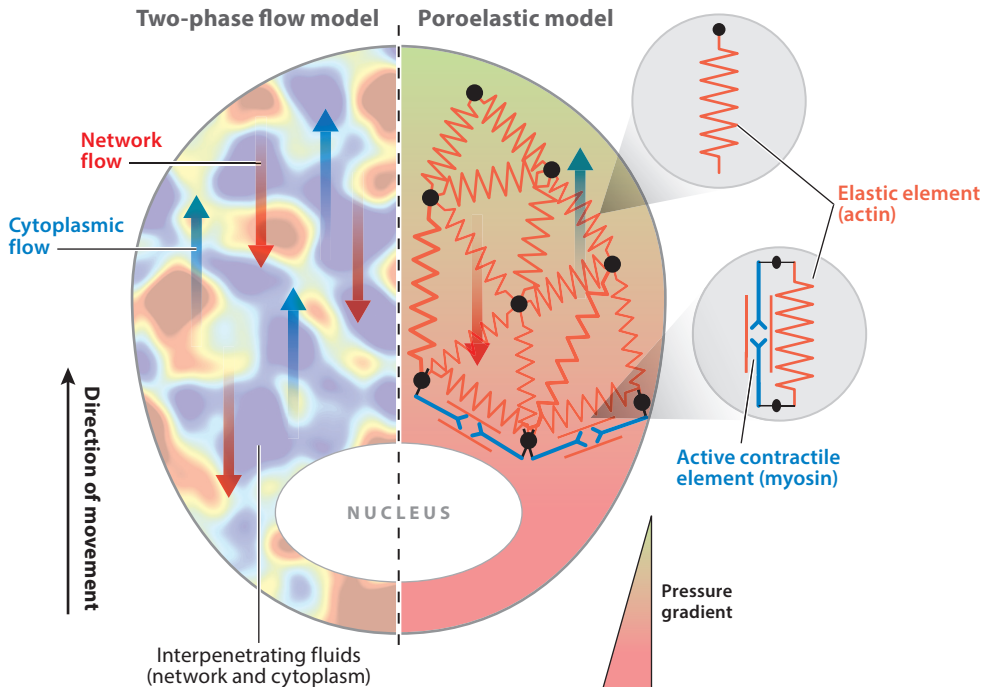


Figure 4

Poroviscoelastic and poroelastic flows in moving cells. In the two-phase flow model (*left*), both the cytoskeletal (*red*) and cytosolic (*blue*) phases are described as fluids that are interpenetrative (*background shading*), but in general, they flow in opposite directions (*red and blue arrows*). In the poroelastic model (*right*), the cytoskeletal network is described as a discrete mesh of elastic spring elements, with actin in *red*, and active contractile elements, with myosin in *dark blue*. The background shading represents the pressure gradient in the cytoskeletal fluid (with *red* representing high, and *green* representing low), which causes the fluid components to flow toward the front (*blue arrow*), whereas the network flows toward the rear (*red arrow*).

FULL COMPLEXITY: TWO-PHASE POROVISCOUS MODEL

There are a lot of experimental data showing that the cytosol flows through the cytoskeletal mesh as opposed to simply sticking to it (**Figure 4**). Therefore, rigorously speaking, to adequately describe the cell mechanics, there must be two sets of equations: one describing the cytoskeletal deformations and another the cytosol fluid dynamics. Mathematically, the easiest case is the one in which the cytosol's behavior is determined by the cytoskeletal dynamics and the feedback from the fluid flow to the polymer mesh is omitted. There are rough estimates (Rubinstein et al. 2009) proposing that this is the case in the lamellipodium, where the actin network is dense, highly cross-linked, and under great myosin contractile stress. Keren et al. (2009) considered the broad, flat, fan-shaped lamellipodium of a motile fish keratocyte, shown in **Figure 2a**, and assumed that actomyosin contraction at the rear of the cell creates a high hydrostatic pressure. They explored various spatial distributions of the membrane permeability to water, solved the Darcy flow equation for the cytosol creeping through the porous actin network, and found that if the membrane is highly permeable at the leading edge, then the myosin-generated pressure creates a fluid flow from the rear to the front of the lamellipodium (**Figure 2a**).

Interestingly, some reports did suggest that aquaporin channels that drastically increase the membrane permeability to water concentrate in functionally important regions of the cell surface

(Hu & Verkman 2006, Loitto et al. 2002). It is impossible to measure the flow in the cytoskeleton-filled cell volume because fluorescent markers have to be so small to flow freely through the nanometer-scale pores that their random diffusion would obscure the directed drift. Thus, to test the prediction that the cytosol in the motile cell flows forward, Keren et al. (2009) solved a reaction-diffusion-drift equation for inert particles in the lamellipodium, where the drift of the particles is generated by the predicted cytosol flow, and found their spatial distribution. Using fluorescent quantum dots with known diffusion coefficients, they measured the distribution of the quantum dots, which compared very well with the predicted distribution.

Estimates showed that the predicted hydrostatic pressure generated by myosin and accompanying the cytosol flow did not contribute significantly to the force pushing the leading edge membrane forward. However, the Péclet number turned out to be comparable to 1, and hence the flow was predicted to assist diffusion in recycling of important proteins from the rear to the front of the cell. In fact, there is experimental evidence that directed convection does move actin monomers to the front of the lamellipodium in some cells (Zicha et al. 2003).

In general, the mechanical effect of the flow on the cytoskeletal mesh is likely nonnegligible, and considering that on a relatively long timescale the actomyosin mesh can be considered as a viscous fluid, the logical way to formulate the mechanics problem is to use the two-phase (poroviscous) flow theory. One of the earliest formulations of this theory, relevant to biological applications, can be found in a study by Drew & Segel (1971) and a review by Cogan & Guy (2010). Credit for practical development and application of this theory to the cell goes to Micah Dembo and coworkers who added the active contractile and swelling stresses and passive drag between the cytoskeleton and the substrate to the standard force balance equations as well as the chemical reaction terms to the conservation equations (Dembo & Harlow 1986). Many studies of the Dembo group were applied to modeling cell motility (Alt & Dembo 1999, Kuusela & Alt 2009).

Characteristic poroviscous theory in one dimension consists of the mass conservation equations for the network,

$$\underbrace{\frac{\partial \varphi}{\partial t} + \frac{\partial}{\partial x}(\varphi u)}_{\text{rate of change of network volume fraction}} = \underbrace{J}_{\text{net rate of assembly/disassembly}},$$

and for the cytosol,

$$\underbrace{\frac{\partial(1-\varphi)}{\partial t} + \frac{\partial}{\partial x}((1-\varphi)v)}_{\text{rate of change of cytosol volume fraction}} = \underbrace{-J}_{\text{net rate of assembly/disassembly}},$$

and of the force balance equations for the network,

$$\underbrace{-\varphi \frac{\partial p}{\partial x}}_{\text{pressure}} - \underbrace{\frac{\partial \Psi}{\partial x}}_{\text{contraction/swelling of polymer gel}} + \underbrace{\frac{\partial}{\partial x}\left(\mu \frac{\partial u}{\partial x}\right)}_{\text{gel viscosity}} = \underbrace{k(u-v)}_{\text{network-cytosol drag}} + \underbrace{\zeta u}_{\text{adhesion drag}},$$

and for the cytosol,

$$\underbrace{-(1-\varphi) \frac{\partial p}{\partial x}}_{\text{pressure}} = \underbrace{k(u-v)}_{\text{network-cytosol drag}}.$$

Here φ is the network volume fraction; u and v are velocities of the network and cytosol, respectively; p is the cytosol pressure; Ψ is the contractile/swelling stress; μ is the network viscosity; k is the network-cytosol drag coefficient; and ζ is the network-surface drag coefficient. These

equations are complemented by the constitutive relations for the reaction term, so that J , Ψ , μ , k , and ζ are functions of φ .

One characteristic example is the application to what is essentially one large, multinucleate cell, the slime mold *Physarum* (Allen & Allen 1978). Fast fluid flow was observed in the center of the cell, flowing from the rear to the front. Dembo & Harlow (1989) solved the equations of the poroviscous theory, adding a hypothetical signaling molecule activated at the cell boundary and diffusing and deactivated in the cytoplasm. Along the central axis of the cell, where this molecule's concentration is low, the cytoskeletal density is low and the cytosol flow rate is high. The solution showed that the cytoskeleton contracts at the rear and the periphery, slowly dragging the cytosol to the rear, and then the fluid escapes rapidly to the front along the cell center, similar to a fountain flow. Another example is the spectacular in silico 3D reproduction of a neutrophil moving inside a cylindrical channel (Herant et al. 2003). By introducing an inhomogeneous adhesion between the cell and channel walls, Herant and coworkers showed that even in the absence of contraction, the cytoskeletal gel swelling at the front generates rearward network flow in the cell framework that exerts traction forces on the channel walls and propels the cell forward.

The poroviscous flow theory is not limited to actin-based cell movements. Nematode sperm cells use a different protein, Major Sperm Protein (MSP), and no molecular motors to generate crawling motility (Zajac et al. 2008). Zajac and coworkers solved the poroviscous theory equation for MSP gel contracting at the rear and swelling at the front of the cell, coupled to cytosol mechanics. The authors assumed that the cell membrane is permeable to water. The solution showed that, in the framework of the cell, the cytoskeleton moves rearward and drags the cytosol with it (**Figure 4**). Consequently, water seeps into the cell at the leading edge and exits at the rear, creating a high hydrostatic pressure at the front. In fact, according to the estimate by Zajac et al. (2008), this pressure is high enough to contribute almost half of the protrusion force (the other half being contributed by the MSP polymerization force).

A very insightful analysis of the poroviscous model of cell motility was done by Kimpton et al. (2013) and Oliver et al. (2005). In 2005, Oliver and coworkers had considered the dorsoventral (vertical) cross section of the cell, much like Kruse et al. (2006), and like Dembo & Harlow (1989) used reaction-diffusion of a signaling molecule that is activated at the cell membrane, is deactivated away from it, and governs the equilibrium network volume fraction. This guaranteed the finite height of the cell in the model. Careful asymptotic analysis using thin-film theory (and the fact that the height of the motile appendage is normally much smaller than its length and width) reduced the model from 2D to 1D allowing for detailed analysis and numerical simulations. Linear stability analysis predicted the formation of ruffles, oscillations of the cell thickness, corresponding to regions of high or low network density. Further, the model explored the highly nontrivial contact line boundary conditions at the front and rear, similar to those in wetting problems for droplets on solid surfaces. Interestingly, a recent experimental study suggested that such boundary conditions could explain the shape and speed of keratocytes (Gabella et al. 2014). In a follow-up study, Kimpton et al. (2015) performed an analysis of the 1D model with a special form of contractile stress: contraction of the actomyosin network at intermediate and swelling at low and high network densities. It showed that mathematically the motile cell is a stable traveling wave with the polymer network flowing to the rear and the cytosol to the front. Curiously, the mathematics predicted that a few sharp peaks of actin density are possible inside the cell.

The two-phase porous model was recently integrated with the polar active gel theory by considering the active nematic network phase to be embedded in the cytosol isotropic phase. Because of the interplay between the active stresses and the geometry of the network polarization, this theory predicted spontaneous division and motility of the cell (Callan-Jones & Jülicher 2011, Giomi & DeSimone 2014). The two-phase porous model was applied to other cell mechanical phenomena

as well; for example, He & Dembo (1997) simulated cytokinesis, the process of cell division, due to the cytoskeletal contraction at the equator of the initially spherical cell. Recently, the role of the cytosolic flow in cytokinesis was further explored by Zhao & Wang (2016) and Zheng et al. (2007).

WHAT IS THE RIGHT RHEOLOGY? THE POREOELASTIC MODEL

On long timescales, the cytoskeletal mechanical behavior is dominated by viscous flows, but exactly what the threshold is at which the short-term elastic responses cross over to the long-term viscous dynamics is not clear and depends on the system being considered. The actin mesh is a mixture of different structures, some of which likely become viscous on a scale of seconds and others on a much longer scale of minutes. Also, a scale of seconds is relevant to some phenomena of fast cell motility, like blebs. Thus, the mechanics of an elastic or elastoviscous cytoskeleton have to be explored.

The idea that gel mechanics can be described by an elastic mesh immersed into the viscous fluid flowing through the pores in the gel mesh is well established and has long been explored mathematically (Biot 1941, Keener et al. 2011, Tanaka & Fillmore 1979). Thirty years ago in a pioneering study, Zhu & Skalak (1988) proposed a model in which a motile pseudopod was considered as a porous solid actin network with pores full of aqueous solution. The driving force of the extension was hypothesized to be provided by the actin polymerization, giving rise to a pressure drop in the fluid phase at the tip of the pseudopod (**Figure 4**). The resulting pressure gradient along the pseudopod was shown to drive the fluid filtration through the actin gel according to Darcy's law and to bring actin monomers to the growing tip.

One of the first computational models of motile poroelastic cells (Bottino & Faucci 1998) considered a 2D actin cytoskeleton represented as a network of nodes linked by elastic elements and surrounded by the cell membrane as an impermeable boundary. The contraction of the network was modeled via the resting length, and the stiffness of the network elastic links was varied in space and time. Use of the immersed boundary method led to the prediction that the cell can move effectively by squeezing fluid into the weakened front from the contracting rear, and adjusting adhesions in sync.

Recently, Guy and collaborators (Lewis et al. 2015, Strychalski et al. 2015) significantly advanced the immersed boundary method to specifically study cell motility within the framework of poroelastic models and applied the method to simulate the motility of *Physarum*. Based on observations of peristaltic waves of contraction and flow in these large cells, the group assumed the contractile force driving the deformation of the cell to be a traveling sinusoidal wave. Numerical simulations revealed that a phase shift between the contractile wave and periodic changes in adhesion strength is the key to directional locomotion. Another notable application of the poroelastic model to *Physarum* is the study by Guy et al. (2011), who used the Brinkman equation instead of Darcy's law, because in some regions of the cell, the volume fraction of polymer is very low and the macroscale viscous stresses are relevant. The important result of this study is that upon introduction to the model of the very plausible assumption that the frictional force from the fluid increases the depolymerization rate of the polymer network, a flow channel along the central axis of the cell evolves, as observed experimentally.

Experimental and theoretical works on the blebs (Charras et al. 2005, 2008; Mitchison et al. 2008) represent the most exciting recent development of the poroelastic theory of cell mechanics. In these pioneering studies, local application of myosin-inhibiting drugs was used to show that the hydrostatic pressure generated by contraction generates blebs locally because the pressure does not equilibrate across cells on time- and length scales relevant to motility (**Figure 1b**). The proposed model was that the cytoskeleton is an elastic, fluid-filled sponge in which the hydrostatic pressure does not instantaneously propagate through the network.

Indeed, characteristic poroelastic theory in one dimension consists of the mass conservation equation

$$(1 - \varphi)v = -\varphi \frac{\partial u}{\partial t},$$

where u is the displacement of the elastic network, and of the force balance equations for the network,

$$\frac{\partial}{\partial x} \left(K \frac{\partial}{\partial x} - (1 - \varphi)p \right) + \frac{\partial \Psi}{\partial x} = 0,$$

where K is the elastic bulk modulus of the network, and for the cytosol,

$$k(1 - \varphi) \left(v - \frac{\partial u}{\partial t} \right) = -\frac{\partial p}{\partial x}.$$

All other variables and parameters have the same meaning as those in the poroviscous theory. Using the equation of continuity in Darcy's law and substituting the result into the force balance yields the diffusion equation for the displacement in the network:

$$\frac{\partial u}{\partial t} = D \frac{\partial^2 u}{\partial x^2} + \frac{1}{k} \frac{\partial \Psi}{\partial x},$$

where the effective diffusion coefficient is a function of the elasticity and permeability of the gel network. Charras et al. (2005) estimated that for realistic network properties in the cell, mechanical perturbations spread over tens of microns in ten seconds.

The conclusions of this theory were experimentally tested. Rosenbluth et al. (2008) used atomic force microscopy to poke the cell and measured resulting displacements. They observed an immediate response but also slower equilibration, occurring over times that increase with increasing distance from the perturbation. This distance-dependent equilibration could be eliminated by the disruption of the actin cytoskeleton. Modeling showed that the experimental results could not be explained by traditional viscoelastic models of cell mechanics, but they were consistent with predictions from a poroelastic description, which accounts for both fast propagation of stress through the solid phase (cytoskeleton) and a much slower diffusive equilibration of hydrostatic pressure of the fluid phase (cytosol). Results from local mechanical perturbations of cells in conjunction with chemical and genetic treatments (Charras et al. 2009, Moeendarbary et al. 2013) led to similar conclusions.

Charras and coworkers used only scaling arguments to estimate the pressure propagation across the cell. By contrast, a recent study by Strychalski & Guy (2016) numerically simulated a cell filled with the discrete elastic cytoskeletal mesh bathed in the cytosol, with the contractile cortex adhering to the elastic membrane at the cell boundary (**Figure 3**). By locally breaking the adhesions and performing numerical experiments mimicking the experimental assays, Strychalski & Guy showed that hydrostatic pressure disturbances from the bleb initiation propagated faster than the timescale of bleb expansion, and that global hydrostatic pressure equilibrated more slowly than the timescale (tens of seconds) of bleb expansion (**Figure 3b**). These multiple timescales in intracellular pressure dynamics explained the apparent discrepancy in the interpretation of the experimental results of Charras et al. (2005) and Tinevez et al. (2009).

THE PROBLEM OF THE BOUNDARY IN CELL MECHANICS

So far, we have focused this review on what happens in the cell bulk. However, note that the dynamic boundary of the cell presents special challenges. One problem stems from the physics of

the plasma membrane enveloping the cell (Alberts et al. 2014). Physically, the membrane's lipid bilayer (a few nanometers thick) behaves as an incompressible and nonstretchable viscous fluid in the membrane's plane (Phillips et al. 2013). However, the membrane behaves similarly to an elastic solid resisting bending when deformed normal to its plane. A great volume of biophysical literature is devoted to the physics of the membrane, membrane vesicles (Bloom et al. 1991), and membrane-bound cell organelles (Terasaki et al. 2013). In motile cells, the membrane is dramatically bent, for example, at the leading cell edge, but estimates show that the bending forces are typically negligible compared to the intracellular force pushing on the membrane and to membrane tension (Kozlov & Mogilner 2007). However, as is often the case in cell biology, one can find examples of systems where every imaginable limiting case is realized; there are many studies in which the Helfrich Hamiltonian that fully accounts for the membrane physics was used to describe the cell boundary mechanics (Atilgan et al. 2006).

In most 2D models of cell motility discussed in this review, the membrane is represented as an elastic, 1D contour that can be thought of as a simple, linear chain of springs. A more sophisticated boundary condition was used by Woolley et al. (2014) that idealized the membrane and cortex as an axisymmetric elastic shell surrounding pressurized cytosol and used large deformation theory to capture the dynamic blebbing morphology. The membrane is often underlined by the actin cortex as well as being folded, stapled by cytoskeletal elements, and rapidly remodeled by endo- and exocytosis (Gauthier et al. 2012). Due to all these complexities, the question about physical and mathematical boundary conditions for cell mechanical models remains open.

The membrane not only provides the mechanical barrier for the cytoskeleton, but its flow is also important in cell motility. When the cell crawls forward, the membrane must translocate in the same direction. One of the possible translocation mechanisms consists of endocytosis at the cell rear, intracellular anterograde transport of the membrane vesicles, and exocytosis at the front (Bretscher & Aguado-Velasco 1998). However, it is also possible that the membrane simply flows forward. A 2D Stokes equation for incompressible viscous fluids describes this flow, with the in-plane membrane tension playing the role of an inverse pressure, the gradient of which drives the flow (Fogelson & Mogilner 2014). Actin pushing at the leading edge creates a membrane tension that is slightly higher than that at the rear, which is sufficient to generate a net forward membrane flow with a rate similar to the cell speed at a characteristic density of transmembrane proteins bound to the actin cortex. These proteins are effectively stationary buoys in the laboratory coordinate system that resist the membrane flow around them. Numerical solutions of the corresponding Stokes equation showed that a membrane tension gradient of ~ 10 pN/ μm across the cell length is sufficient to drive this flow in rapidly moving keratocytes (Fogelson & Mogilner 2014, Schweitzer et al. 2014). This prediction was confirmed experimentally by measuring the membrane tension at the front and rear of the moving cells (Lieber et al. 2015).

The problem of membrane flow becomes more complicated if the cytosol and the fluid outside the cell are also moving. A calculation of the flows inside, within and outside a lipid vesicle (Woodhouse & Goldstein 2012) demonstrated that the constraint of lateral incompressibility of the membrane leads to a significant reduction in the membrane flow. Another complication for the problem of membrane flows is the presence of a great number of mobile membrane proteins embedded in the lipid bilayer. Sigurdsson & Atzberger (2016) used the immersed boundary method to solve the 2D Stokes equation on the curved membrane surface with inclusion particles coupled through intramembrane hydrodynamics. They found that the membrane curvature and topology augment hydrodynamic responses, leading to interesting coordinated motions of the membrane proteins.

One mathematically interesting feature of many problems concerned with moving or dividing cells is that the motile cell is a free boundary object, in which deformations of the cell shape

depend on, and in turn affect, the actin-myosin and cytosol movements and forces inside the cell. The history of the free-boundary cell modeling was recently reviewed by Holmes & Edelstein-Keshet (2012). Related to the 2D lamellipodia, the free boundary problem was first introduced by Rubinstein et al. (2005), who posited that the spatially graded centripetal actin flow retracts the lamellipodial boundary. Actin growth at the boundary results in protrusion that counteracts the retraction, and a balance of protrusion and retraction shapes the lamellipodium, feeding back to the actin-myosin contraction in the bulk of the 2D lamellipodium, described above.

A few models successfully reproduced the characteristic keratocyte shape by solving partial differential equations for the 2D actin-myosin mechanics and advancing the boundary point-by-point (Barnhart et al. 2015) or more rigorously by using either level-set methods (Wolgemuth et al. 2011), phase-field methods (Shao et al. 2010, Ziebert & Aranson 2013, Ziebert et al. 2011), or the immersed boundary method (Vanderlei et al. 2011). Interestingly, completely different models based on a reaction-diffusion of regulatory molecules and using Potts models (energy minimization) with a free boundary also reproduced the motile keratocyte shape (Marée et al. 2006, Nishimura & Sasai 2007). The free boundary models were used recently to explore complex effects of dynamic and nonhomogeneous adhesions (Barnhart et al. 2015, Shao et al. 2010, Ziebert & Aranson 2013). Three-dimensional free boundary models of varying sophistication were also developed and reproduced an impressive diversity of the cell motile morphologies in higher dimensions (Herant & Dembo 2010, Tjhung et al. 2015, Tozluoğlu et al. 2013, Zhu & Mogilner 2016).

FUTURE CHALLENGES

Mathematical and computational studies of the last decades have led to basic understanding of the cell mechanics. We should, however, be under no illusion: We have just scratched the tip of the iceberg of cellular complexity, and we are in the dark about the majority of mechanics-related cell biological phenomena. Understanding the behavior of the mechanical cell presents mathematical, modeling, and computational challenges not encountered in more traditional mechanics, because of the stochastic, multiscale, and multicomponent nature of the cell. Among the greatest future challenges will be, first, to formulate stochastic mathematical models of cell mechanics (Atzberger et al. 2007), which are needed due to the small number of copies of some impermanent cytoskeletal elements with random dynamics. Second, a challenge stems from the fact that the cytoskeleton is not a simple viscoelastic material but is characterized by nonlinear stress-strain relations with memory and elements of plasticity (MacKintosh & Schmidt 2010). In fact, in some cases, the cytoskeleton could be better described as a glassy material than a visco-elasto-plastic continuum (Fabry et al. 2001). Also, constitutive relations for the mechanical models have to be derived from very complex molecular mechanics. One characteristic example is the stick-slip drag between the cytoskeleton and the surface on which the cell moves (Barnhart et al. 2015, Sabass et al. 2008), which stems from the force-dependent rate of adhesion molecule detachment (Chan & Odde 2008). Another related problem is that the cytoskeleton-cytosol mixture is, in fact, a strong, not diluted, polyelectrolyte (Janmey et al. 2014), and understanding of mechanics equations for such materials is still sketchy. Third, the cytoskeleton is highly anisotropic and heterogeneous; even more important, it is a mixture of drastically different types of polymer-motor networks. One ubiquitous example is that linear stress fibers are very often embedded into the 3D mesh of a branched actin network, which is bounded by the dense 2D actin cortex (Alberts et al. 2014).

Fourth, as if mechanics were not complicated enough by themselves, cell mechanical phenomena are intimately coupled to biochemical and, on a longer timescale, gene regulation dynamics (Iglesias & Devreotes 2012, Shivashankar 2011). Fifth, the free boundary nature of many cell biological processes, with nontrivial physics of the plasma membrane at the boundary, presents

another level of computational difficulties. Last but not least, the main thrust of the experimental cell motility research has recently started to shift from studying cells on flat, rigid surfaces to investigating physiologically relevant cell migration through 3D deformable extracellular matrices. Computationally, this means that the deformable mechanics of the medium into which the cell is embedded must be added to the model (Tozluoğlu et al. 2013, Zhu & Mogilner 2016). The rheology of the extracellular matrices is no less complex than that of the cytoskeleton (Liu et al. 2016, Marquez et al. 2005).

Most important of all, however, will be to better integrate experimental and theoretical efforts. Currently, mathematical papers on cell mechanics deal with difficult computational problems but rarely attempt to become a truly predictive tool for specific experimental systems. On one hand, elegant physical papers often limit themselves to semiquantitative estimates and do not address geometric and mechanical complexity. Experimental papers, on the other hand, often use insightful yet simplistic mechanical analogies. Unity of mathematical sophistication, physical insight, and quantitative biological data is the key to overcoming the challenges of understanding fluid mechanics of the cell.

DISCLOSURE STATEMENT

The authors are not aware of any biases that might be perceived as affecting the objectivity of this review.

ACKNOWLEDGMENTS

This work was supported by the US Army Research Office 70744-MA to A.M. We thank C. Copos for useful discussions.

LITERATURE CITED

- Alberts B, Johnson A, Lewis J, Morgan D, Raff M, et al. 2014. *Molecular Biology of the Cell*. New York: Garland Sci. 6th ed.
- Allen GM, Mogilner A, Theriot JA. 2013. Electrophoresis of cellular membrane components creates the directional cue guiding keratocyte galvanotaxis. *Curr. Biol.* 23(7):560–68
- Allen RD, Allen NS. 1978. Cytoplasmic streaming in amoeboid movement. *Annu. Rev. Biophys. Bioeng.* 7(1):469–95
- Alt W, Dembo M. 1999. Cytoplasm dynamics and cell motion: two-phase flow models. *Math. Biosci.* 156(1):207–28
- Atilgan E, Wirtz D, Sun SX. 2006. Mechanics and dynamics of actin-driven thin membrane protrusions. *Biophys. J.* 90(1):65–76
- Atzberger PJ, Kramer PR, Peskin CS. 2007. A stochastic immersed boundary method for fluid-structure dynamics at microscopic length scales. *J. Comput. Phys.* 224(2):1255–92
- Barnhart E, Lee KC, Allen GM, Theriot JA, Mogilner A. 2015. Balance between cell–substrate adhesion and myosin contraction determines the frequency of motility initiation in fish keratocytes. *PNAS* 112(16):5045–50
- Bausch AR, Kroy K. 2006. A bottom-up approach to cell mechanics. *Nat. Phys.* 2(4):231–38
- Bausch AR, Ziemann F, Boulbitch AA, Jacobson K, Sackmann E. 1998. Local measurements of viscoelastic parameters of adherent cell surfaces by magnetic bead microrheometry. *Biophys. J.* 75(4):2038–49
- Bergert M, Chandradoss SD, Desai RA, Paluch E. 2012. Cell mechanics control rapid transitions between blebs and lamellipodia during migration. *PNAS* 109(36):14434–39
- Biot MA. 1941. General theory of three-dimensional consolidation. *J. Appl. Phys.* 12(2):155–64

- Bloom M, Evans E, Mouritsen OG. 1991. Physical properties of the fluid lipid-bilayer component of cell membranes: a perspective. *Q. Rev. Biophys.* 24(3):293–397
- Bottino DC, Fauci LJ. 1998. A computational model of ameiboid deformation and locomotion. *Eur. Biophys. J.* 27(5):532–39
- Bretscher MS, Aguado-Velasco C. 1998. Membrane traffic during cell locomotion. *Curr. Opin. Cell Biol.* 10(4):537–41
- Brugués J, Nuzzo V, Mazur E, Needleman DJ. 2012. Nucleation and transport organize microtubules in metaphase spindles. *Cell* 149(3):554–64
- Callan-Jones AC, Jülicher F. 2011. Hydrodynamics of active permeating gels. *New J. Phys.* 13(9):093027
- Carlier MF, Romet-Lemonne G, Jegou A. 2014. Actin filament dynamics using microfluidics. *Methods Enzymol.* 540:3–17
- Carlsson AE. 2011. Mechanisms of cell propulsion by active stresses. *New J. Phys.* 13(7):073009
- Chan CE, Odde DJ. 2008. Traction dynamics of filopodia on compliant substrates. *Science* 322(5908):1687–91
- Charras GT, Coughlin M, Mitchison TJ, Mahadevan L. 2008. Life and times of a cellular bleb. *Biophys. J.* 94(5):1836–53
- Charras GT, Mitchison TJ, Mahadevan L. 2009. Animal cell hydraulics. *J. Cell Sci.* 122(18):3233–41
- Charras GT, Yarrow JC, Horton MA, Mahadevan L, Mitchison TJ. 2005. Non-equilibration of hydrostatic pressure in blebbing cells. *Nature* 435(7040):365–69
- Cogan NG, Guy RD. 2010. Multiphase flow models of biogels from crawling cells to bacterial biofilms. *HFSP J.* 4(1):11–25
- Dai J, Sheetz MP. 1999. Membrane tether formation from blebbing cells. *Biophys. J.* 77(6):3363–70
- Dembo M. 1989. Mechanics and control of the cytoskeleton in *Amoeba proteus*. *Biophys. J.* 55(6):1053–80
- Dembo M, Harlow F. 1986. Cell motion, contractile networks, and the physics of interpenetrating reactive flow. *Biophys. J.* 50(1):109–21
- Díz-Muñoz A, Romanczuk P, Yu W, Bergert M, Ivanovitch K, et al. 2016. Steering cell migration by alternating blebs and actin-rich protrusions. *BMC Biol.* 14(1):74
- Drew DA, Segel LA. 1971. Averaged equations for two-phase flows. *Stud. Appl. Math.* 50(3):205–31
- Eloy C, Lauga E. 2012. Kinematics of the most efficient cilium. *Phys. Rev. Lett.* 109(3):038101
- Fabry B, Maksym GN, Butler JP, Glogauer M, Navajas D, Fredberg JJ. 2001. Scaling the microrheology of living cells. *Phys. Rev. Lett.* 87(14):148102
- Fogelson B, Mogilner A. 2014. Computational estimates of membrane flow and tension gradient in motile cells. *PLOS ONE* 9(1):e84524
- Gabella C, Bertseva E, Bottier C, Piacentini N, Bornert A, et al. 2014. Contact angle at the leading edge controls cell protrusion rate. *Curr. Biol.* 24(10):1126–32
- Gauthier NC, Masters TA, Sheetz MP. 2012. Mechanical feedback between membrane tension and dynamics. *Trends Cell Biol.* 22(10):527–35
- Giomi L, DeSimone A. 2014. Spontaneous division and motility in active nematic droplets. *Phys. Rev. Lett.* 112(14):147802
- Goldstein RE. 2016. Fluid dynamics at the scale of the cell. *J. Fluid Mech.* 807:1–39
- Goldstein RE, van de Meent JW. 2015. A physical perspective on cytoplasmic streaming. *Interface Focus* 5(4):20150030
- Gracheva ME, Othmer HG. 2004. A continuum model of motility in ameboid cells. *Bull. Math. Biol.* 66(1):167–93
- Gross SP, Welte MA, Block SM, Wieschaus EF. 2000. Dynein-mediated cargo transport in vivo: A switch controls travel distance. *J. Cell Biol.* 148(5):945–56
- Guy RD, Nakagaki T, Wright GB. 2011. Flow-induced channel formation in the cytoplasm of motile cells. *Phys. Rev. E* 84(1):016310
- He X, Dembo M. 1997. On the mechanics of the first cleavage division of the sea urchin egg. *Exp. Cell Res.* 233(2):252–73
- Hecht I, Rappel WJ, Levine H. 2009. Determining the scale of the Bicoid morphogen gradient. *PNAS* 106(6):1710–15
- Herant M, Dembo M. 2010. Form and function in cell motility: from fibroblasts to keratocytes. *Biophys. J.* 98(8):1408–17

- Herant M, Marganski WA, Dembo M. 2003. The mechanics of neutrophils: synthetic modeling of three experiments. *Biophys. J.* 84(5):3389–413
- Holmes WR, Edelstein-Keshet L. 2012. A comparison of computational models for eukaryotic cell shape and motility. *PLOS Comput. Biol.* 8(12):e1002793
- Hu J, Verkman AS. 2006. Increased migration and metastatic potential of tumor cells expressing aquaporin water channels. *FASEB J.* 20(11):1892–94
- Iglesias PA, Devreotes PN. 2012. Biased excitable networks: how cells direct motion in response to gradients. *Curr. Opin. Cell Biol.* 24(2):245–53
- Iskratsch T, Wolfenson H, Sheetz MP. 2014. Appreciating force and shape—the rise of mechanotransduction in cell biology. *Nat. Rev. Mol. Cell Biol.* 15(12):825–33
- Jaeger M, Carin M, Medale M, Tryggvason G. 1999. The osmotic migration of cells in a solute gradient. *Biophys. J.* 77(3):1257–67
- Janmey PA, Slochower DR, Wang YH, Wen Q, Cébers A. 2014. Polyelectrolyte properties of filamentous biopolymers and their consequences in biological fluids. *Soft Matter* 10(10):1439–49
- Joanny JF, Prost J. 2009. Active gels as a description of the actin-myosin cytoskeleton. *HFSP J.* 3(2):94–104
- Kamm RD. 2002. Cellular fluid mechanics. *Annu. Rev. Fluid Mech.* 34(1):211–32
- Keener JP, Sircar S, Fogelson AL. 2011. Kinetics of swelling gels. *SIAM J. Appl. Math.* 71(3):854–75
- Keren K, Yam PT, Kinkhabwala A, Mogilner A, Theriot JA. 2009. Intracellular fluid flow in rapidly moving cells. *Nat. Cell Biol.* 11(10):1219–24
- Khismatullin DB, Truskey GA. 2012. Leukocyte rolling on P-selectin: a three-dimensional numerical study of the effect of cytoplasmic viscosity. *Biophys. J.* 102(8):1757–66
- Kimpton LS, Whiteley JP, Waters SL, King JR, Oliver JM. 2013. Multiple travelling-wave solutions in a minimal model for cell motility. *Math. Med. Biol.* 30(3):241–72
- Kimpton LS, Whiteley JP, Waters SL, Oliver JM. 2015. On a poroviscoelastic model for cell crawling. *J. Math. Biol.* 70(1–2):133–71
- Kole TP, Tseng Y, Jiang I, Katz JL, Wirtz D. 2005. Intracellular mechanics of migrating fibroblasts. *Mol. Biol. Cell* 16(1):328–38
- Kozlov MM, Mogilner A. 2007. Model of polarization and bistability of cell fragments. *Biophys. J.* 93(11):3811–19
- Kruse K, Joanny JF, Jülicher F, Prost J. 2006. Contractility and retrograde flow in lamellipodium motion. *Phys. Biol.* 3(2):130
- Kruse K, Joanny JF, Jülicher F, Prost J, Sekimoto K. 2004. Aster, vortices, and rotating spirals in active gels of polar filaments. *Phys. Rev. Lett.* 92(7):078101
- Kruse K, Joanny JF, Jülicher F, Prost J, Sekimoto K. 2005. Generic theory of active polar gels: a paradigm for cytoskeletal dynamics. *Eur. Phys. J. E* 16(1):5–16
- Kuusela E, Alt W. 2009. Continuum model of cell adhesion and migration. *J. Math. Biol.* 58(1–2):135–61
- Larripa K, Mogilner A. 2006. Transport of a 1D viscoelastic actin–myosin strip of gel as a model of a crawling cell. *Physica A* 372(1):113–23
- Lee P, Wolgemuth CW. 2011. Crawling cells can close wounds without purse strings or signaling. *PLOS Comput. Biol.* 7(3):e1002007
- Lewis OL, Guy RD, Allard JF. 2014. Actin–myosin spatial patterns from a simplified isotropic viscoelastic model. *Biophys. J.* 107(4):863–70
- Lewis OL, Zhang S, Guy RD, del Álamo JC. 2015. Coordination of contractility, adhesion and flow in migrating *Physarum* amoebae. *J. R. Soc. Interface* 12(106):20141359
- Li Y, Mori Y, Sun SX. 2015. Flow-driven cell migration under external electric fields. *Phys. Rev. Lett.* 115(26):268101
- Lieber AD, Schweitzer Y, Kozlov MM, Keren K. 2015. Front-to-rear membrane tension gradient in rapidly moving cells. *Biophys. J.* 108(7):1599–603
- Lim FY, Chiam KH, Mahadevan L. 2012. The size, shape, and dynamics of cellular blebs. *Europhys. Lett.* 100(2):28004
- Lim FY, Koon YL, Chiam KH. 2013. A computational model of amoeboid cell migration. *Comput. Methods Biomech. Biomed. Eng.* 16(10):1085–95

- Liu AS, Wang H, Copeland CR, Chen CS, Shenoy VB, Reich DH. 2016. Matrix viscoplasticity and its shielding by active mechanics in microtissue models: experiments and mathematical modeling. *Sci. Rep.* 6:33919
- Loitto VM, Forslund T, Sundqvist T, Magnusson KE, Gustafsson M. 2002. Neutrophil leukocyte motility requires directed water influx. *J. Leukoc. Biol.* 71(2):212–22
- Luby-Phelps K. 1999. Cytoarchitecture and physical properties of cytoplasm: volume, viscosity, diffusion, intracellular surface area. *Int. Rev. Cytol.* 192:189–221
- Luby-Phelps K. 2013. The physical chemistry of cytoplasm and its influence on cell function: an update. *Mol. Biol. Cell* 24(17):2593–96
- MacKintosh FC, Schmidt CF. 2010. Active cellular materials. *Curr. Opin. Cell Biol.* 22(1):29–35
- Marée AF, Jilkine A, Dawes A, Grieneisen VA, Edelstein-Keshet L. 2006. Polarization and movement of keratocytes: a multiscale modelling approach. *Bull. Math. Biol.* 68(5):1169–211
- Marquez JP, Genin GM, Zahalak GI, Elson EL. 2005. The relationship between cell and tissue strain in three-dimensional bio-artificial tissues. *Biophys. J.* 88(2):778–89
- Mitchison TJ, Charras GT, Mahadevan L. 2008. Implications of a poroelastic cytoplasm for the dynamics of animal cell shape. *Semin. Cell Dev. Biol.* 19(3):215–23
- Moeendarbary E, Valon L, Fritzsche M, Harris AR, Moulding DA, et al. 2013. The cytoplasm of living cells behaves as a poroelastic material. *Nat. Mater.* 12(3):253–61
- Monteith CE, Brunner ME, Djagaeva I, Bielecki AM, Deutsch JM, Saxton WM. 2016. A mechanism for cytoplasmic streaming: kinesin-driven alignment of microtubules and fast fluid flows. *Biophys. J.* 110(9):2053–65
- Nishimura SI, Sasai M. 2007. Modulation of the reaction rate of regulating protein induces large morphological and motional change of amoebic cell. *J. Theor. Biol.* 245(2):230–37
- Oakes PW, Banerjee S, Marchetti MC, Gardel ML. 2014. Geometry regulates traction stresses in adherent cells. *Biophys. J.* 107(4):825–33
- Oliver JM, King JR, McKinlay KJ, Brown PD, Grant DM, et al. 2005. Thin-film theories for two-phase reactive flow models of active cell motion. *Math. Med. Biol.* 22(1):53–59
- Oster GF, Perelson AS. 1987. The physics of cell motility. *J. Cell Sci.* 1987(Suppl. 8):35–54
- Paluch EK, Raz E. 2013. The role and regulation of blebs in cell migration. *Curr. Opin. Cell Biol.* 25(5):582–90
- Peskin CS, McQueen DM. 1995. A general method for the computer simulation of biological systems interacting with fluids. *Symp. Soc. Exp. Biol.* 49:265–76
- Petrie RJ, Koo H, Yamada KM. 2014. Generation of compartmentalized pressure by a nuclear piston governs cell motility in a 3D matrix. *Science* 345(6200):1062–65
- Phillips R, Kondev J, Theriot J, Garcia HG. 2013. *Physical Biology of the Cell*. New York: Garland Sci. 2nd ed.
- Pollack GH. 2001. *Cells, Gels and the Engines of Life: A New, Unifying Approach to Cell Function*. Seattle: Ebner
- Prass M, Jacobson K, Mogilner A, Radmacher M. 2006. Direct measurement of the lamellipodial protrusive force in a migrating cell. *J. Cell Biol.* 174(6):767–72
- Quinlan ME. 2016. Cytoplasmic streaming in the *Drosophila* oocyte. *Annu. Rev. Cell Dev. Biol.* 32:173–95
- Recho P, Putelat T, Truskovsky L. 2013. Contraction-driven cell motility. *Phys. Rev. Lett.* 111(10):108102
- Robinson DN, Spudich JA. 2004. Mechanics and regulation of cytokinesis. *Curr. Opin. Cell Biol.* 16(2):182–88
- Rosenbluth MJ, Crow A, Shaevitz JW, Fletcher DA. 2008. Slow stress propagation in adherent cells. *Biophys. J.* 95(12):6052–59
- Rotsch C, Jacobson K, Radmacher M. 1999. Dimensional and mechanical dynamics of active and stable edges in motile fibroblasts investigated by using atomic force microscopy. *PNAS* 96(3):921–26
- Rubinstein B, Fournier MF, Jacobson K, Verkhovsky AB, Mogilner A. 2009. Actin-myosin viscoelastic flow in the keratocyte lamellipod. *Biophys. J.* 97(7):1853–63
- Rubinstein B, Jacobson K, Mogilner A. 2005. Multiscale two-dimensional modeling of a motile simple-shaped cell. *Multiscale Model. Simul.* 3(2):413–39
- Sabass B, Gardel ML, Waterman CM, Schwarz US. 2008. High resolution traction force microscopy based on experimental and computational advances. *Biophys. J.* 94(1):207–20
- Schwarz US. 2015. Physical constraints for pathogen movement. *Semin. Cell Dev. Biol.* 46:82–90
- Schweitzer Y, Lieber AD, Keren K, Kozlov MM. 2014. Theoretical analysis of membrane tension in moving cells. *Biophys. J.* 106(1):84–92

- Shao D, Rappel WJ, Levine H. 2010. Computational model for cell morphodynamics. *Phys. Rev. Lett.* 105(10):108104
- Sheetz MP, Sable JE, Döbereiner HG. 2006. Continuous membrane-cytoskeleton adhesion requires continuous accommodation to lipid and cytoskeleton dynamics. *Annu. Rev. Biophys. Biomol. Struct.* 35:417–34
- Shinar T, Mana M, Piano F, Shelley MJ. 2011. A model of cytoplasmically driven microtubule-based motion in the single-celled *Caenorhabditis elegans* embryo. *PNAS* 108(26):10508–13
- Shivashankar GV. 2011. Mechanosignaling to the cell nucleus and gene regulation. *Annu. Rev. Biophys.* 40:361–78
- Sigurdsson JK, Atzberger PJ. 2016. Hydrodynamic coupling of particle inclusions embedded in curved lipid bilayer membranes. *Soft Matter* 12(32):6685–707
- Stroka KM, Jiang H, Chen SH, Tong Z, Wirtz D, et al. 2014. Water permeation drives tumor cell migration in confined microenvironments. *Cell* 157(3):611–23
- Strychalski W, Copos CA, Lewis OL, Guy RD. 2015. A poroelastic immersed boundary method with applications to cell biology. *J. Comput. Phys.* 282:77–97
- Strychalski W, Guy RD. 2012. A computational model of bleb formation. *Math. Med. Biol.* 30(2):115–30
- Strychalski W, Guy RD. 2016. Intracellular pressure dynamics in blebbing cells. *Biophys. J.* 110(5):1168–79
- Tanaka T, Fillmore DJ. 1979. Kinetics of swelling of gels. *J. Chem. Phys.* 70(3):1214–18
- Tao J, Li Y, Vig DK, Sun SX. 2017. Cell mechanics: a dialogue. *Rep. Prog. Phys.* 80(3):036601
- Terasaki M, Shemesh T, Kasthuri N, Klemm RW, Schalek R, et al. 2013. Stacked endoplasmic reticulum sheets are connected by helicoidal membrane motifs. *Cell* 154(2):285–96
- Tinevez JY, Schulze U, Salbreux G, Roensch J, Joanny JF, Paluch E. 2009. Role of cortical tension in bleb growth. *PNAS* 106(44):18581–86
- Tjhung E, Tiribocchi A, Marenduzzo D, Cates ME. 2015. A minimal physical model captures the shapes of crawling cells. *Nat. Commun.* 6:5420
- Tozluoglu M, Tournier AL, Jenkins RP, Hooper S, Bates PA, Sahai E. 2013. Matrix geometry determines optimal cancer cell migration strategy and modulates response to interventions. *Nat. Cell Biol.* 15(7):751–62
- Trong PK, Doerflinger H, Dunkel J, St. Johnston D, Goldstein RE. 2015. Cortical microtubule nucleation can organise the cytoskeleton of *Drosophila* oocytes to define the anteroposterior axis. *eLife* 4:e06088
- Vanderlei B, Feng JJ, Edelstein-Keshet L. 2011. A computational model of cell polarization and motility coupling mechanics and biochemistry. *Multiscale Model. Simul.* 9(4):1420–43
- Weirich KL, Banerjee S, Dasbiswas K, Witten TA, Vaikuntanathan S, Gardel ML. 2017. Liquid behavior of cross-linked actin bundles. *PNAS* 114(9):2131–36
- Wolgemuth CW, Stajic J, Mogilner A. 2011. Redundant mechanisms for stable cell locomotion revealed by minimal models. *Biophys. J.* 101(3):545–53
- Wolke U, Jezuit EA, Priess JR. 2007. Actin-dependent cytoplasmic streaming in *C. elegans* oogenesis. *Development* 134(12):2227–36
- Wollman R, Civelekoglu-Scholey G, Scholey JM, Mogilner A. 2008. Reverse engineering of force integration during mitosis in the *Drosophila* embryo. *Mol. Syst. Biol.* 4(1):195
- Woodhouse FG, Goldstein RE. 2012. Shear-driven circulation patterns in lipid membrane vesicles. *J. Fluid Mech.* 705:165–75
- Woolley TE, Gaffney EA, Oliver JM, Baker RE, Waters SL, Goriely A. 2014. Cellular blebs: pressure-driven, axisymmetric, membrane protrusions. *Biomech. Model. Mechanobiol.* 13(2):463–76
- Xie J, Hu GH. 2016. Hydrodynamic modeling of Bicoid morphogen gradient formation in *Drosophila* embryo. *Biomech. Model. Mechanobiol.* 15(6):1765–73
- Yi K, Unruh JR, Deng M, Slaughter BD, Rubinstein B, Li R. 2011. Dynamic maintenance of asymmetric meiotic spindle position through Arp2/3-complex-driven cytoplasmic streaming in mouse oocytes. *Nat. Cell Biol.* 13(10):1252–58
- Young J, Mitran S. 2010. A numerical model of cellular blebbing: a volume-conserving, fluid–structure interaction model of the entire cell. *J. Biomech.* 43(2):210–20
- Zajac M, Dacanay B, Mohler WA, Wolgemuth CW. 2008. Depolymerization-driven flow in nematode spermatozoa relates crawling speed to size and shape. *Biophys. J.* 94(10):3810–23

- Zhao J, Wang Q. 2016. A 3D multi-phase hydrodynamic model for cytokinesis of eukaryotic cells. *Commun. Comput. Phys.* 19(03):663–81
- Zheng F, Basciano C, Li J, Kuznetsov AV. 2007. Fluid dynamics of cell cytokinesis—numerical analysis of intracellular flow during cell division. *Int. Commun. Heat Mass Transf.* 34(1):1–7
- Zhu CH, Skalak RI. 1988. A continuum model of protrusion of pseudopod in leukocytes. *Biophys. J.* 54(6):1115–37
- Zhu J, Mogilner A. 2016. Comparison of cell migration mechanical strategies in three-dimensional matrices: a computational study. *Interface Focus* 6(5):20160040
- Zicha D, Dobbie IM, Holt MR, Monypenny J, Soong DY, et al. 2003. Rapid actin transport during cell protrusion. *Science* 300(5616):142–45
- Ziebert F, Aranson IS. 2013. Effects of adhesion dynamics and substrate compliance on the shape and motility of crawling cells. *PLOS ONE* 8(5):e64511
- Ziebert F, Swaminathan S, Aranson IS. 2011. Model for self-polarization and motility of keratocyte fragments. *J. R. Soc. Interface* 9(70):1084–92
- Zumdieck A, Voituriez R, Prost J, Joanny JF. 2008. Spontaneous flow of active polar gels in undulated channels. *Faraday Discuss.* 139:369–75